

Modal Dynamic Response of a Darreius Wind Turbine Rotor with NACA0018 Blade Profile

Soumia Benbouta

Laboratoire de Mecanique des Structures et Materiaux, Universite Batna 2, Batna, 05000, Algeria
soumia.benbouta@univ-batna2.dz (corresponding author)

Toufik Outtas

Laboratoire de Mecanique des Structures et Materiaux, Universite Batna 2, Batna, 05000, Algeria
t.outtas@univ-batna2.dz

Fateh Ferroudji

Unite de Recherche en Energies Renouvelables en Milieu Saharien, URERMS, Centre de Developpement des Energies Renouvelables, CDER, 01000, Adrar, Algeria
fferroudji@yahoo.fr

Received: 23 November 2024 | Revised: 20 December 2024 and 2 January 2025 | Accepted: 6 January 2025

Licensed under a CC-BY 4.0 license | Copyright (c) by the authors | DOI: <https://doi.org/10.48084/etasr.9697>

ABSTRACT

The global wind energy industry achieved a significant milestone by reaching a total capacity of one terawatt (TW) by the end of 2023, underscoring the increasing importance of wind energy as a sustainable energy source (Global Wind Energy Outlook, 2022). This study focuses on the simulation and dynamic analysis of an H-Darrieus wind turbine rotor using 3D Finite Element Analysis (FEA). Key structural parameters, including natural frequencies, associated vibration modes, and mass participation rates, were determined to optimize the rotor performance. A novel blade design is proposed in this work, offering a lighter and more robust alternative to traditional rotor blades manufactured from composites, like fiberglass-polyester, fiberglass-epoxy, or combinations with wood and carbon. The lighter design enhances the startup performance at low wind speeds, while the improved strength and fixing mechanisms ensure resilience against the increasingly severe sandstorms reported in recent years. The vibration dynamics of the rotor under critical wind loads were analyzed using the SolidWorks Simulation software, yielding highly satisfactory results. The stability and reliability of the rotor were validated, as the dynamic performance indices, and the quality criteria meet the requirements for optimal operation.

Keywords-modal dynamic; H-Darrieus wind turbine; CAD; 3D modeling; finite element analysis

I. INTRODUCTION

Wind power is projected to remain a pivotal renewable energy source in the global electricity mix for the foreseeable future [1, 2]. Following solar energy, wind power has undergone significant development over the past decade and is now one of the most sought-after renewable energy technologies [3]. Vertical Axis Wind Turbines (VAWTs) possess distinct advantages, including insensitivity to wind direction, fewer components, low noise emissions, and a robust three-dimensional structural design. These features make VAWTs a viable alternative to traditional Horizontal Axis Wind Turbines (HAWTs), especially in scenarios where adaptability to turbulent wind conditions, aesthetic integration, and noise reduction are priorities [1].

In recent years, VAWTs have gained popularity for use in urban and semi-urban areas due to their insensitivity to wind direction, low cut-in wind speed, simpler construction, and

reduced noise and fatigue concerns. Their installation on the ground or atop buildings is straightforward and cost-effective [4, 5]. VAWTs come in various configurations, including lift-driven Darrieus rotors with curved or straight blades and drag-driven Savonius rotors. Among these, the straight-bladed H-type Darrieus turbine, invented by G. Darrieus in 1931, stands out for its simple design and reliable operation [6, 7]. The structural and aerodynamic design of turbine blades plays a crucial role in optimizing power output, extending lifespan, and reducing costs [8, 9]. However, under extreme environmental conditions -including aerodynamic, centrifugal, and gravitational loads- the blade structure must be capable of operating safely and reliably over a lifespan of up to 20 years [10, 11].

Several numerical and analytical studies of the dynamic behavior of straight, three-bladed rotors in H-Darrieus Wind Turbines (HDWTs) have been recently carried out. For example, authors in [12] conducted structural strength analyses

using FEA techniques to fabricate straight blades made from aluminum and galvanized steel for a 2.5 kW Savonius-Darrieus turbine. Furthermore, in [13], a 3D FEA simulation was performed to determine the modal behavior -natural frequencies and associated mode shapes- of a 10 kW H-type Darrieus turbine blade made from aluminum. Using a simplified model, authors in [14] developed an analytical technique to study the vibration of an H-type VAWT. Experimental methods were employed in [15] to investigate the modal response of a VAWT installed on a building. Additionally, authors in [16] proposed vibration control methods for VAWTs, while authors in [17] explored the impact of turbine speed on the VAWT dynamic behavior. Despite these contributions, the vibrational properties of VAWTs are often overlooked. A review of the literature reveals a limited number of studies on free and forced vibration analyses of VAWTs, with the exception of [14–17]. This highlights a significant gap in understanding the vibrational behavior of these systems.

The present work aims to address this gap by investigating the free and forced vibrations of H-type VAWTs. To the best of the authors' knowledge, no comparative studies have been published on this subject. Mastering the design and operation of this type of wind turbine is crucial for enabling the cost-effective, local manufacturing of wind turbines capable of supplying electricity to rural populations far from conventional grids. The objective of this study is to numerically simulate the forced vibrations of a newly designed blade for a three-bladed H-Darrieus wind turbine. SolidWorks, a highly efficient FEA software, is used to conduct numerical simulations.

II. PROCEDURE FOR MODELING THE ROTOR OF THE NACA0018 WIND TURBINE WITH SOLIDWORKS SOFTWARE

Computer-Aided Design (CAD) has become an indispensable tool in the design and manufacturing of technical systems. It enables the materialization of design calculations, the evaluation of new or existing systems using simulation tools, and the implementation of modifications without incurring additional expenses. For this study, the SolidWorks design software was employed. The modeling process began with the design of the individual components of the H-Darrieus rotor, including the blades, the central axis for securing the blades, and the blade/mast attachment arms. Once the components were designed, they were assembled to create the full rotor structure, as shown in Figure 1. The primary technical specifications of the rotor for the H-Darrieus wind turbine are summarized in Table I.

The system under study is a vertical-axis wind turbine of the H-Darrieus type with a 10-kW power output. This wind turbine operates as an electromechanical converter, transforming the wind energy into mechanical or electrical energy through lift. The three-blade rotor is designed to capture a portion of the wind's kinetic energy and convert it into mechanical energy. This mechanical energy is subsequently transformed into electrical energy using a MADA (Double-Powered Asynchronous Machine) generator. The wind turbine consists of three primary components: a fixed part which includes a hollow circular mast, an intermediate part which

houses the MADA generator, and a rotating part comprising the H-Darrieus rotor. The rotor entails three blades attached to three supports arms, which in turn are connected to the central rotating mast. The entire wind turbine structure is mounted on a reinforced concrete foundation with anchor rods for stability, as displayed in Figure 1.

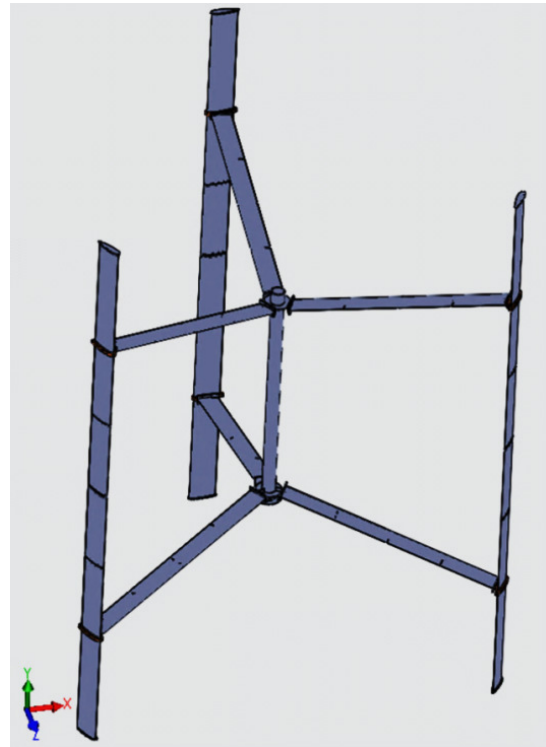


Fig. 1. Complete assembly of the wind turbine rotor.

TABLE I. MAIN TECHNICAL CHARACTERISTICS OF THE WIND TURBINE ROTOR

Parameter	Unit	Value
Power Generated	kW	10
Rated wind speed	m/s	10
Rotation speed	tr/min	60
Cut-in wind speed	m/s	3
Cut-out wind speed	m/s	19
Swept area	m ²	63.5
Rotor diameter, D	m	7.2
Rotor height, H	m	8.8
Blade airfoil	-	NACA 0018
Blades number, N	-	3
Chord length, c	mm	400
Blade material	-	Aluminum alloy

A. Elements of Assembly

The modeling of the wind turbine rotor components was accomplished using SolidWorks, as illustrated in Figure 2. Partial assemblies of the wind turbine rotor are depicted in Figures 3- 5.

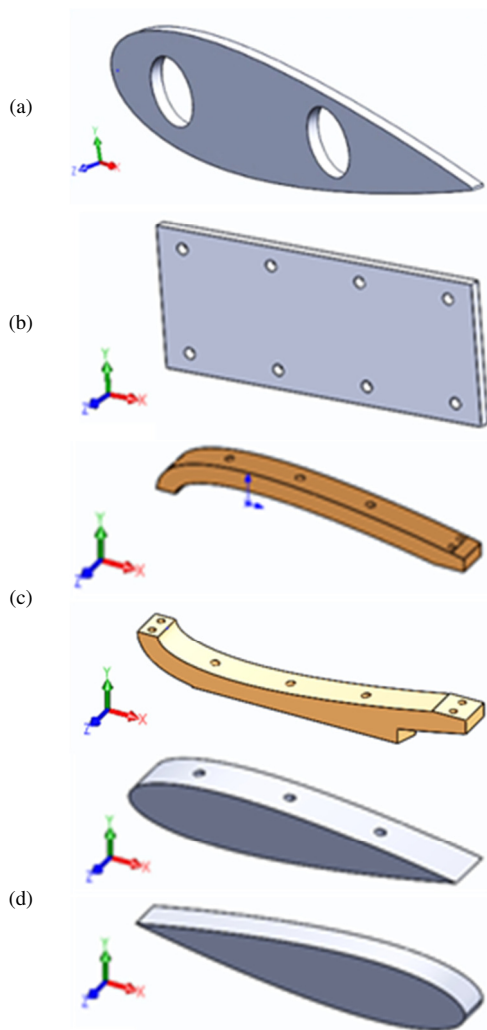


Fig. 2. Parts of the windturbine rotor: (a) blade support plate, (b) crown/blade fixing element, (c) arm/blade fixing reinforcement, (d) internal fixing element for blade parts.

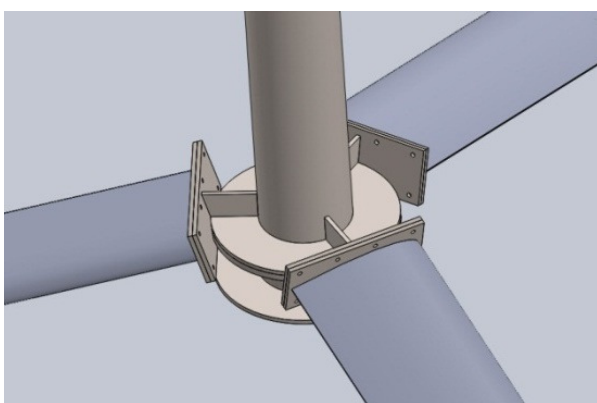


Fig. 3. Partial assembly of the wind turbine rotor.

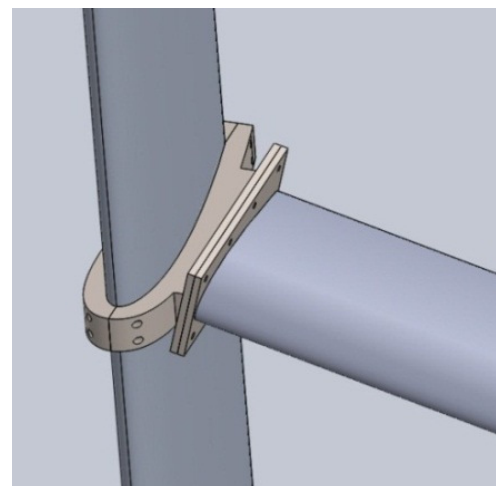


Fig. 4. Detail of arm/blade fixing reinforcement system.

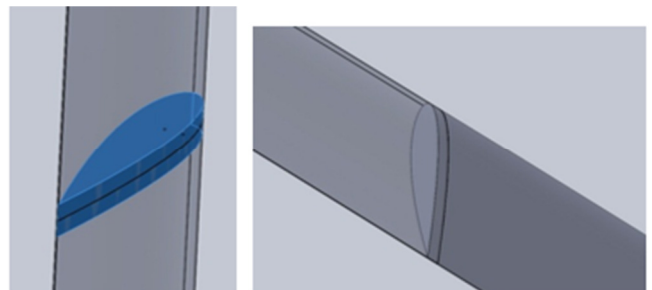


Fig. 5. Detail of internal fixing element of blade parts.

B. Material Used

The material used for the FEA was selected from the SolidWorks Simulation library to match those of the rotor structure. The blades were designed using an aluminum alloy, chosen for its lightweight and structural strength. The central axis for fixing the blades and arms, as well as the connecting bars, was made of stainless steel (AISI 1020 steel, cold-rolled) due to its durability and mechanical properties. The materials and their properties used in the FEA model are detailed in Table II [18].

TABLE II. MECHANICAL PROPERTIES OF WIND TURBINE ROTOR CONSTRUCTION MATERIALS

Properties	AISI 1020 steel	Aluminum alloy
Modulus of Elasticity (GPa)	200	69
Poisson Coefficient	0.29	0.33
Yield Strength (MPa)	351.57	27.57
Density (kg/m ³)	7870	2700

III. FINITE ELEMENT ANALYSIS OF WIND TURBINE ROTOR STRUCTURE

The FEA of the wind turbine rotor structure was conducted using SolidWorks Simulation, one of the most widely utilized software tools in mechanical design and related fields [19]. The FEA process in SolidWorks Simulation involves three primary stages: preprocessing, analysis, and post-processing. The key components of the FEA model include: a Finite Element (FE) mesh, material properties, external loads, boundary conditions,

and a geometric model of the structure, developed in SolidWorks.

A. Meshing the Wind Turbine Rotor Model on SolidWorks

The studied rotor features a volumetric structure, which was meshed using tetrahedral elements. SolidWorks automatically generated a mixed mesh for the wind turbine rotor's volumetric components. To minimize numerical errors, well-proportioned FEs were utilized to refine the mesh along the rotor's height. The final FE model comprises 147,585 elements and 72,983 nodes, as portrayed in Figures 6 and 7.

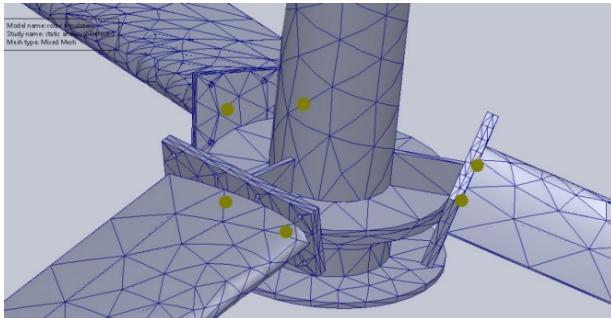


Fig. 6. Meshing details of fixture system of blade with central axis.

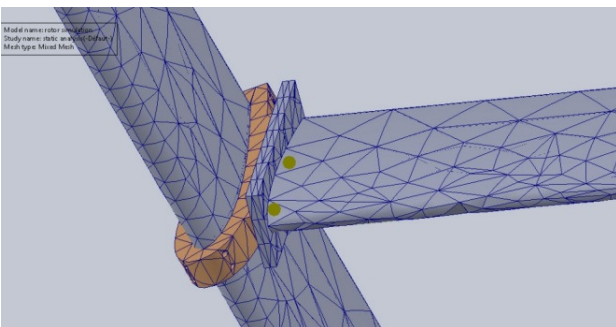


Fig. 7. Meshing details of fixture system of blade with arms.

A summary of the mesh information is provided in Table III.

TABLE III. INFORMATION ON THE OVERALL ROTOR MESH SIZE

Mesh Type	Mixed mesh Shell with 6ddl/node Solid with 3ddl/node (translations)
Max element Size	179.149 mm
Min element Size	35.8298 mm
Quality	high
Number of elements	147585
Number of Nodes	72983
Number of Degrees of Freedom	6ddl/node for shell 3ddl/node for solid

B. Boundary Conditions (Imposed Displacements and Applied Loadings)

Boundary conditions are essential for defining the operational environment of the model. The specified applied loads and imposed displacements significantly influence the

analysis results [20]. In this study, imposed displacements were applied to the six central blade/mast attachment arms. Subsequently, all displacements were constrained (set to zero). These boundary conditions are depicted in Figure 8.

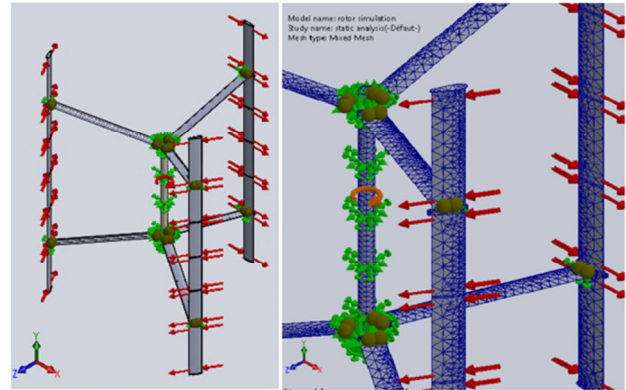


Fig. 8. The imposed displacements and applied loadings.

C. Critical Loading Conditions

The structure of the wind turbine rotor is subject to three primary types of stresses:

- Mechanical stresses, such as gust forces and storm-included loads.
- Thermal stresses, caused by temperature variations.
- Hygrometric stresses, resulting from changes in humidity levels.

For this study, only mechanical loads were considered. The mechanical loads applied during the analysis include:

1) Aerodynamic Loading

The aerodynamic loading on the rotor due to wind is calculated using the equation recommended by IEC 61400-2:2006 [21]:

$$P_x = \frac{1}{2} C_T \rho_{air} V_{wind}^2 \tag{1}$$

where: $C_T = 0.5$ is the trust coefficient [22], $\rho_{air} = 1.225 \text{ kg/m}^3$ is the mass density of air, and V_{wind} is the wind speed in m/s.

2) Centrifugal Force (F_c)

The centrifugal force caused by the turbine's rotation is expressed as:

$$F_c = mR\omega^2 \tag{2}$$

where F_c is the centrifugal force in N, m is the mass of the rotor in kg, ω is the angular speed in rad/s calculated at the four different wind speed values of V_{wind} (in service 10 and 15 and out of service 20 and 25 m/s) and R is the distance (the turbine's radius) between the blade's center of gravity and its axis of rotation. All the results of the aerodynamic loads due to wind on the rotor and centrifugal forces caused by the rotation of the turbine for three different wind speed values are detailed in Table IV.

TABLE IV. AERODYNAMIC WIND LOADS ON THE ROTOR

Wind speed V_{wind} (m/s)	Pressure P_x (N/m ²)	Centrifugal force F_c (kN)
10	30.62	392
15	68.90	882
20	122.50	1568
25	191.40	2450

D. Dynamic Parameters Analysis

The dynamic performance indices of the wind turbine provide insights into its vibration behavior and structural stability. The key parameters analyzed are:

1) Mass Participation Ratio

The Mass Participation Ratio (MPR) SolidWorks Simulation quantifies the proportion of mass participating in the vibration response of the system in each principal direction of the wind turbine structure. It is calculated using SolidWorks Simulation according to [23]:

$$X_{mass,i} = \frac{\sum_{r=1}^n (\ddot{q}_{rX_i})^2}{\sum m_{X_i}}, \quad X_i = X, Y, Z \quad (3)$$

2) Amplification Factor

The amplification factor measures the ratio of total vibration energy to energy lost due to tight connections, internal interactions, dry friction in joints, material hysteresis, viscous damping, and the propagation of acoustic waves lost during the vibration cycle is measured by this indicator. For light-damping structures, this factor typically ranges between 5 and 50, depending on the materials and accessories used.

For metal structures, the vibration mode indicator Q_r can be determined using the formula provided in [24]:

$$Q_r = \frac{1}{\xi_r \sqrt{1 - \xi_r^2}} \cong \frac{1}{2\xi_r} \quad (4)$$

The damping ratio ξ_r for ductile materials can be approximated by [25]:

$$\xi_r = \frac{1}{10 + 0.05\Omega_r} \quad (5)$$

3) Amplitude Ratios of Resonance Modes

The natural frequencies of the structure and the maximum responses are connected since the force, mass, and the damping generalized for all modes are the same [18]:

$$\frac{|A_r|_{max}}{|A_1|_{max}} = \Omega_i^2 \Omega_r^2 \quad (6)$$

4) Excitation Frequencies

The excitation frequencies Ω_f of the wind turbine, induced by wind speeds (m/s), can be expressed as a function of the following parameters : turbine radius $R_t = 3.6$ m, number of blades $N_b = 3$, and specific design speed ratio $\lambda_d = 2.8$. The expression for excitation frequencies is:

$$\Omega_f = \frac{N_b \lambda_d V_w}{2\pi R_t} \quad (7)$$

IV. RESULTS AND DISCUSSION

The simulation results of the first five vibration modes of the wind turbine rotor are presented in Figures 9(a)-9(e) and the simulation results of the modal analysis of the three-blade wind turbine are listed in Tables V and VI.

TABLE V. WIND TURBINE STRUCTURAL CHARACTERISTICS AND QUALITY FACTORS

Mode	Ω_r (Hz)	$V_r = \Omega_r R_t$ (m/s)	MPR			ξ_r (%)	Q_r	$ A_r _m / A_1 _m$ (%)
			X	Y	Z			
1	14.675	52.830	1.64E-2	6.82E-12	5.47E-3	9.31	5.3705	100.0000
2	14.79	53.244	1.61E-2	9.26E-10	5.39E-3	9.31	5.3720	98.4509
3	14.882	53.575	1.22E-9	2.28E-12	2.22E-2	9.30	5.3763	97.2374
4	16.792	61.099	1.11E-4	6.96E-3	6.94E-4	9.21	5.4288	74.7635
5	16.792	61.099	2.22E-3	2.87E-4	5.26E-3	9.21	5.4288	74.7635
34	33.792	121.651	1.16E-3	2.19E-2	4.14E-4	8.54	5.8548	18.7952
43	46.769	168.368	1.85E-18	2.24E-19	5.96E-19	8.10	6.1728	9.8455
67	70.515	253.854	4.33E-3	1.84E-09	1.29E-05	7.39	6.7658	4.3310

TABLE VI. EXCITATION FREQUENCIES IN HERTZ OF THE WIND TURBINE DUE TO TSR AND WIND SPEEDS

$V_w \backslash \lambda_d$	1.5	2	2.5	2.8	3	3.5	4	4.5
5	0.994	1.326	1.657	1.856	1.989	2.321	2.652	2.984
10	1.989	2.652	3.315	3.713	3.978	4.642	5.305	5.968
15	2.984	3.978	4.973	5.570	5.968	6.963	7.957	8.952
20	3.978	5.305	6.631	7.427	7.957	9.284	10.610	11.936
25	4.973	6.631	8.281	9.284	9.947	11.605	13.262	14.920
30	5.968	7.957	9.947	11.140	11.936	13.926	15.915	17.804
35	6.963	9.284	11.605	12.997	13.926	16.247	18.568	20.889
40	7.957	10.610	13.262	14.854	15.915	18.568	21.220	23.873
45	8.952	11.936	14.920	16.711	17.904	20.889	23.873	26.857
50	9.947	13.262	16.578	18.568	19.894	23.210	26.525	29.841

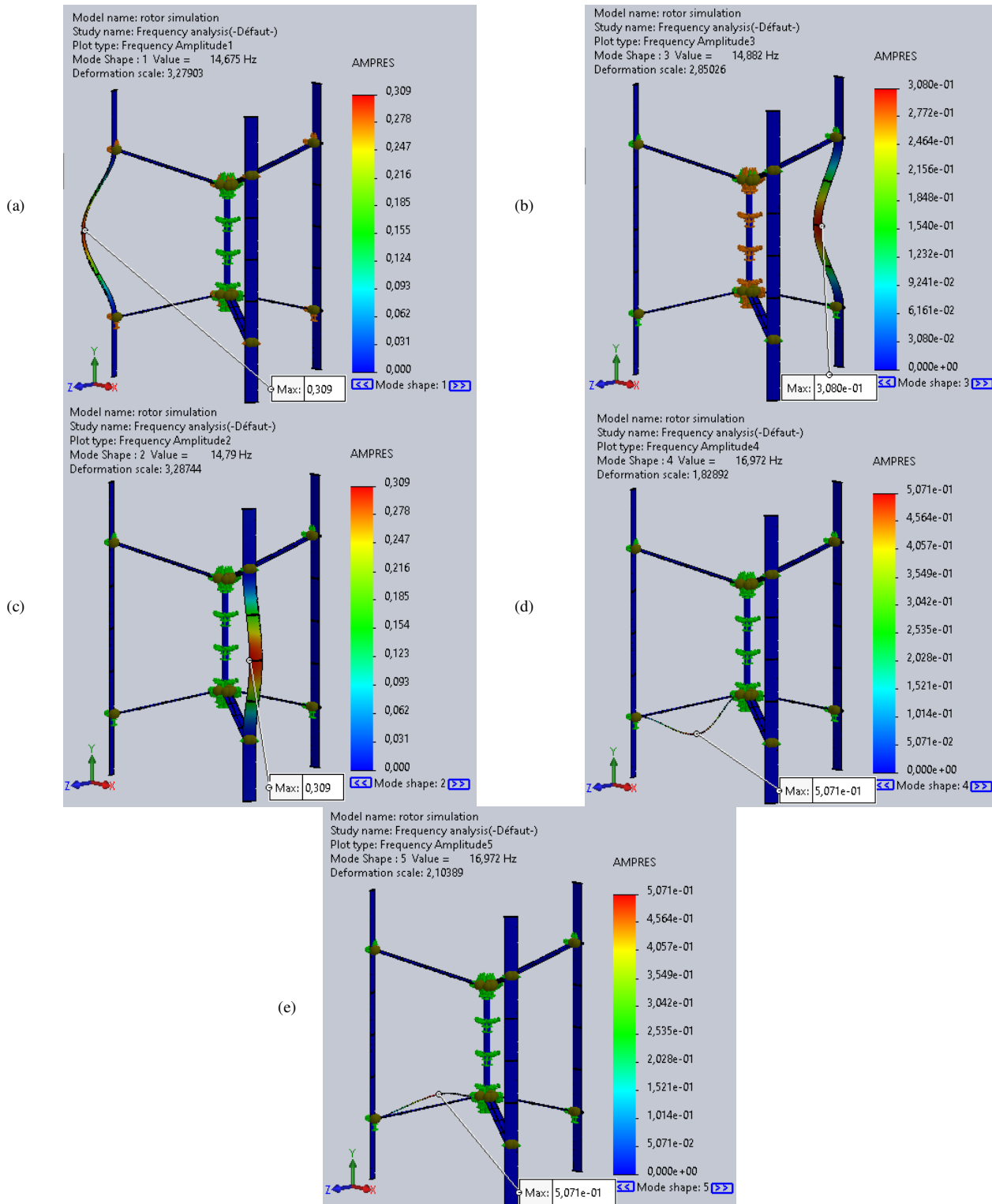


Fig. 9. The first five mode shapes.

The results of the simulation of the 3D FEA of the three-blade H-Darrieus wind provide valuable insights into its dynamic behavior and structural characteristics. The key findings are:

- The first three bending modes of the blades occur at natural frequencies of approximately 14.675 Hz, 14.79 Hz, and 14.88 Hz, as evidenced in Figure 9. These frequencies arise

from the structural symmetry of the turbine in the X and Z directions.

- For the bending vibration modes, these results align with the basic vibration theory of a Euler-Bernoulli beam with lumped masses.
- The symmetrical responses observed in Figures 9(a)-9(c) show that the blades exhibit bending primarily in the X and Z directions.
- In the fourth and fifth modes, as can be seen in Figures 9(d) and 9(e), the blades remain straight, while the structure demonstrates bending in the lower arms in the Z direction. These modes are observed at a natural frequency of 16.97 Hz.

Frequency versus the cumulative effective mass participation factor is presented in Figure 10.

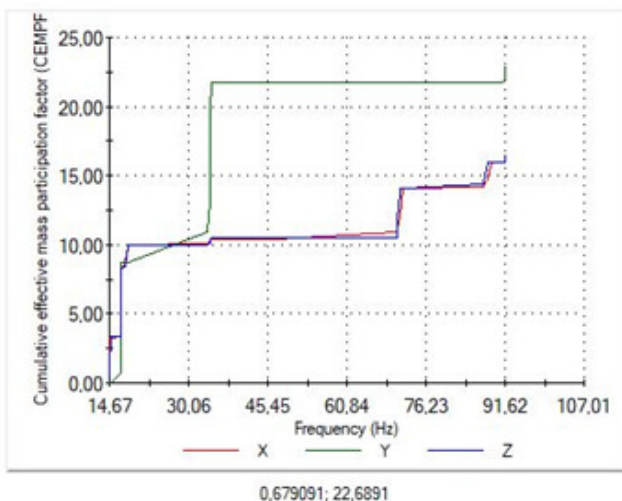


Fig. 10. Frequency versus cumulative effective mass participation factor.

- The MPR is negligible for the first three modes in the Y direction but becomes significant for the fourth and fifth modes, as displayed in Figure 10.
- The MPR significantly influences the first and second bending modes in the X direction, as well as the third bending mode in the Z direction, with the latter showing an MPR of approximately 2.2%.
- Table V highlights that the vibration modes are associated with wind speeds between 52.83 m/s and 61.09 m/s for the first five modes. For higher modes (e.g., modes 34, 43, and 67), the wind speeds range from 121.65 to 253.85 m/s.
- As natural frequencies increase, the corresponding resonant amplitudes decline significantly beyond the 34th mode. This indicates a stable and reliable dynamic response in accordance with the structural dynamics standards.
- The amplification factor Q_r progressively increases with natural frequency, peaking at $Q_r = Q_r$, where resonance occurs. The maximum Q_r based on the simulation results,

does not exceed 7, indicating that the HDWT is a lightly damp structure.

- Table VI reveals that the HDWT exhibits a dense clustering of natural vibration frequencies between 14 Hz and 17 Hz, with a tip-speed ratio (TSR) of approximately 2.8.
- Dangerous excitation frequencies, 14.92 Hz and 16.71 Hz, emerge at wind speeds of 40 m/s and 45 m/s, respectively, corresponding to a TSR of 2.8.
- The reference wind speed for the Adrar region, Algeria (Wind Zone II), does not exceed 28 m/s [26]. At this wind speed, the HDWT structure remains free from resonance issues.
- If the turbine operates at wind speeds above 28 m/s, effective control mechanisms are required to mitigate deformations and dynamic stresses, and thus ensure structural safety and functionality.

V. CONCLUSIONS

This study focused on the simulation and modal dynamic analysis of the rotor structure of a three bladed H-Darrieus wind turbine using the SolidWorks software. The modal simulation and analysis enabled a detailed evaluation of the structure, identifying its optimal structural parameters including the frequencies, the associated natural modes and the rates of mass participation of the structure free from any stress, which are essential for mitigating dynamic resonance. The findings validate the structural stability and reliability of the wind turbine rotor, as all tested dynamic quality criteria align with established standards in the field of structural dynamics. These results demonstrate the suitability of the rotor design for safe operation under typical wind conditions. To enhance performance, this work proposed a novel blade design for the H-Darrieus vertical-axis rotor, achieving a balance between reduced weight and increased robustness. This advancement represents a significant contribution to the rotor technology, potentially improving its efficiency and durability.

Future efforts should focus on experimentally validating the numerical results presented in this study. Such experimental verification would further refine the rotor's structural parameters, leading to enhanced operational reliability and performance of the designed model.

REFERENCES

- [1] N. Batista, R. Melício, and V. Mendes, "Darrieus-type vertical axis rotary-wings with a new design approach grounded in double-multiple streamtube performance prediction model," *AIMS Energy*, vol. 6, no. 5, pp. 673–694, Sep. 2018, <https://doi.org/10.3934/energy.2018.5.673>.
- [2] D. Glasberg, S. Stratila, and I. Malael, "A Numerical Analysis on the Performance and Optimization of the Savonius Wind Turbine for Agricultural Use," *Engineering, Technology & Applied Science Research*, vol. 14, no. 1, pp. 12621–12627, Feb. 2024, <https://doi.org/10.48084/etasr.6543>.
- [3] P. M. Kumar, K. Sivalingam, S. Narasimalu, T.-C. Lim, S. Ramakrishna, and H. Wei, "A Review on the Evolution of Darrieus Vertical Axis Wind Turbine: Small Wind Turbines," *Journal of Power and Energy Engineering*, vol. 7, no. 4, pp. 27–44, Apr. 2019, <https://doi.org/10.4236/jpee.2019.74002>.
- [4] J. Lin, Y. Xu, and Y. Xia, "Structural Analysis of Large-Scale Vertical Axis Wind Turbines Part II: Fatigue and Ultimate Strength Analyses,"

- Energies*, vol. 12, no. 13, Jan. 2019, Art. no. 2584, <https://doi.org/10.3390/en12132584>.
- [5] W. Tjiu, T. Marnoto, S. Mat, M. H. Ruslan, and K. Sopian, "Darrieus vertical axis wind turbine for power generation I: Assessment of Darrieus VAWT configurations," *Renewable Energy*, vol. 75, pp. 50–67, Mar. 2015, <https://doi.org/10.1016/j.renene.2014.09.038>.
- [6] S. Brusca, R. Lanzafame, and M. Messina, "Design of a vertical-axis wind turbine: how the aspect ratio affects the turbine's performance," *International Journal of Energy and Environmental Engineering*, vol. 5, no. 4, pp. 333–340, Dec. 2014, <https://doi.org/10.1007/s40095-014-0129-x>.
- [7] K. Roummani *et al.*, "A new concept in direct-driven vertical axis wind energy conversion system under real wind speed with robust stator power control," *Renewable Energy*, vol. 143, pp. 478–487, Dec. 2019, <https://doi.org/10.1016/j.renene.2019.04.156>.
- [8] M. S. Genç and R. Özkan, "Optimum layer sequence analysis for composite blade using ACP-FSI model," *International Journal of Sustainable Aviation*, vol. 7, no. 4, pp. 354–371, Jan. 2021, <https://doi.org/10.1504/IJSA.2021.119693>.
- [9] C. Kong, J. Bang, and Y. Sugiyama, "Structural investigation of composite wind turbine blade considering various load cases and fatigue life," *Energy*, vol. 30, no. 11, pp. 2101–2114, Aug. 2005, <https://doi.org/10.1016/j.energy.2004.08.016>.
- [10] H. Boudounit, M. Tarfaoui, D. Saifaoui, and M. Nachtane, "Structural analysis of offshore wind turbine blades using finite element method," *Wind Engineering*, vol. 44, no. 2, pp. 168–180, Apr. 2020, <https://doi.org/10.1177/0309524X19849830>.
- [11] C. Muyan and D. Coker, "Finite element simulations for investigating the strength characteristics of a 5&thinspm composite wind turbine blade," *Wind Energy Science*, vol. 5, no. 4, pp. 1339–1358, Oct. 2020, <https://doi.org/10.5194/wes-5-1339-2020>.
- [12] F. Ferroudji and C. Khelifi, "Structural Strength Analysis and Fabrication of a Straight Blade of an H-Darrieus Wind Turbine," *Journal of Applied and Computational Mechanics*, vol. 7, no. 3, pp. 1276–1282, Jul. 2021, <https://doi.org/10.22055/jacm.2020.31452.1876>.
- [13] F. Ferroudji, L. Saihi, and K. Roummani, "Finite Element Modelling and Analysis for Modal Investigation of a Blade H-Type Darrieus Rotor," in *Artificial Intelligence and Renewables Towards an Energy Transition*, Cham, Switzerland, 2021, pp. 416–422, https://doi.org/10.1007/978-3-030-63846-7_39.
- [14] E. Verkinderen and B. Imam, "A simplified dynamic model for mast design of H-Darrieus vertical axis wind turbines (VAWTs)," *Engineering Structures*, vol. 100, pp. 564–576, Oct. 2015, <https://doi.org/10.1016/j.engstruct.2015.06.041>.
- [15] Y. Wang, W. Lu, K. Dai, M. Yuan, and S.-E. Chen, "Dynamic Study of a Rooftop Vertical Axis Wind Turbine Tower Based on an Automated Vibration Data Processing Algorithm," *Energies*, vol. 11, no. 11, Nov. 2018, Art. no. 3135, <https://doi.org/10.3390/en11113135>.
- [16] M. Rahman, Z. C. Ong, W. T. Chong, S. Julai, and S. Y. Khoo, "Performance enhancement of wind turbine systems with vibration control: A review," *Renewable and Sustainable Energy Reviews*, vol. 51, pp. 43–54, Nov. 2015, <https://doi.org/10.1016/j.rser.2015.05.078>.
- [17] I. B. Mabrouk, A. El Hami, L. Walha, B. Zghal, and M. Haddar, "Dynamic vibrations in wind energy systems: Application to vertical axis wind turbine," *Mechanical Systems and Signal Processing*, vol. 85, pp. 396–414, Feb. 2017, <https://doi.org/10.1016/j.ymsp.2016.08.034>.
- [18] F. Ferroudji, C. Khelifi, and F. Meguellati, "Modal analysis of a small H-Darrieus wind turbine based on 3D CAD, FEA," *International Journal of Renewable Energy Research (IJRER)*, vol. 6, no. 2, pp. 637–643, 2016.
- [19] P. M. Kurowski, *Vibration Analysis with SOLIDWORKS Simulation 2016*, Mission, KS, USA: SDC Publications, May 2016.
- [20] M. Chakrouba and F. Ferroudji, "Conception, modélisation statique & fabrication des pales d'éolienne de type Darrieus," Ph.D. Thesis, Université Ahmed Draia-ADRAR, Adrar, Adrar Province, Algeria, 2017.
- [21] *Wind turbines – Part 2: Design requirements for small wind turbines*, 61400-2:2006, IEC, 2006.
- [22] M. A. Biadgo, A. Simonović, D. Komarov, and S. Stupar, "Numerical and analytical investigation of vertical axis wind turbine," *FME transactions*, vol. 41, no. 1, pp. 49–58, 2013.
- [23] E. L. Wilson, *Three dimensional static and dynamic analysis of structures: A physical approach with emphasis on earthquake engineering*, 3rd ed. California, LA, USA: Computers and Structures, Inc., 2002.
- [24] A. Girard and N. Roy, *Structural Dynamics in Industry*. Hoboken, NJ, USA: John Wiley & Sons, 2010.
- [25] G. F. Abdelal, N. Abueffoutouh, and A. Hamdy, "Mechanical fatigue and spectrum analysis of small-satellite structure," *International Journal of Mechanics and Materials in Design*, vol. 4, no. 3, pp. 265–278, Sep. 2008, <https://doi.org/10.1007/s10999-008-9064-4>.
- [26] CNERIB, *Règlement Neige et Vent 1999*, 2000.